

Monte Carlo studies on the long time dynamic properties of dense cubic lattice multichain systems. I. The homopolymeric melt

Andrzej Kolinski,^{a)} Jeffrey Skolnick,^{b)} and Robert Yaris

Institute of Macromolecular Chemistry, Department of Chemistry, Washington University, St. Louis, Missouri 63130

(Received 2 January 1987; accepted 4 March 1987)

Dynamic Monte Carlo simulations of long chains confined to a cubic lattice system at a polymer volume fraction of $\phi = 0.5$ were employed to investigate the dynamics of polymer melts. It is shown that in the range of chain lengths n , from $n = 64$ to $n = 800$ there is a crossover from a weaker dependence of the diffusion coefficient on chain length to a much stronger one, consistent with $D \sim n^{-2}$. Since the n^{-2} scaling relation signals the onset of highly constrained dynamics, an analysis of the character of the chain contour motion was performed. We found no evidence for the well-defined tube required by the reptation model of polymer melt dynamics. The lateral motions of the chain contour are still large even in the case when $n = 800$, and the motion of the chain is essentially isotropic in the local coordinates. Hence, the crossover to the $D \sim n^{-2}$ regime with increasing chain length of this monodisperse model melt is not accompanied by the onset of reptation dynamics.

I. INTRODUCTION

The mechanism of polymer motion in a concentrated solution or in a melt has long been an active area of investigation. By far the most widely accepted model of polymer dynamics is the reptation model of de Gennes,¹⁻³ with the subsequent refinements of Doi and Edwards.⁴ This model asserts that the matrix of chains surrounding the test chain can be treated as fixed with the net result that the dominant long wavelength motion of the test chain is longitudinal; that is, the chain "slithers" out the tube formed by its neighbors. This model predicts that the self-diffusion coefficient D and shear viscosity η depends on degree of polymerization n as n^{-2} and n^3 , respectively. Experimentally, the scaling of D with n has been confirmed⁵⁻¹⁵ but η appears to vary as the 3.4 power of the molecular weight.^{16,17} Moreover, some experiments in concentrated solutions seem to call into question the validity of a simple reptation explanation of self-diffusion.^{15,18} However, as both D and η average over very long wavelength motions, the experiments may be unable to distinguish between reptation and some other motion which provides the same scaling behavior. What in fact is required is a direct examination of the character of the motion itself; unfortunately, direct experimental measurements of this sort are not possible. Thus, we have embarked on a series of computer simulations designed to elucidate the qualitative nature of polymer motion in a melt.^{19,20}

Multichain lattice systems are frequently used as a model of polymer solutions or melts.²¹ Both the statics and dynamics of these simple systems seem to exhibit many of the essential features of real polymeric systems.²² The utility of the lattice approach is that it allows one to study, by computer simulation methods, longer polymers at higher concentrations than are feasible employing more sophisticated models.

It is now well established that the basic equilibrium properties of long lattice chains are the same regardless of lattice details, and change only with dimensionality of the system.²³ However, it is less clear to what extent the same universality holds in the case of time-dependent properties simulated by means of Monte Carlo (MC) lattice dynamics. Having a discrete set of elementary motions is an intrinsic disadvantage of MC lattice dynamics. Thus, in what follows, there is some ambiguity in mapping the polymer volume fraction of the model system onto the density of a real system. However, in spite of these limitations, it is believed that the discrete character of the local motions in a correctly defined MC model should wash out over relatively short distances and that the excluded volume effect and topological constraints emerging from chain entanglements are qualitatively well accounted for.

Recently, we reported the results of dynamic MC studies of multichain diamond lattice systems that covered a wide range of volume fraction ϕ (up to $\phi = 0.75$ for the long time dynamics,²⁰ and up to $\phi \simeq 0.86$ in the case of short time dynamics¹⁹) and chain length (up to $n = 216$ at $\phi = 0.5$). It was shown that there exist a range of densities where the self-diffusion coefficient D and the terminal relaxation time τ_R of the end-to-end vector are consistent with the experimentally observed $D \sim n^{-2 \pm 0.1}$ and $\eta \sim n^{3.4}$ (with the assumption that τ_R is proportional to the viscosity of the melt over the range of n and ϕ studied). Although the number of entanglements per chain estimated for these model systems seemed to satisfy every theoretical requirement for the onset of reptation,²⁴⁻²⁷ detailed analysis of the motion of the equivalent path of the chain (where small distance fluctuations are averaged out and which should be identical to the primitive path of Edwards²⁸), showed the complete absence of a tube. In other words, the dominant long wavelength motion was not longitudinal motion down the primitive path defined at zero time. Rather, the dynamics of the system was closer to a strongly slowed down Rouse-like motion.^{29,30} Therefore, it appears that in these model systems the onset of reptation is

^{a)} Permanent address: Department of Chemistry, University of Warsaw, 02-093 Warsaw, Poland.

^{b)} Alfred P. Sloan Foundation Fellow.

not a necessary condition for the scaling $D \sim n^{-2}$ and $\eta \sim n^{3.4}$. On the contrary, at the very least there is a wide crossover region where reptation-like motions contribute very little to the melt dynamics.

While it is difficult to answer definitively the question of to what extent the lattice restrictions influence the long time dynamics of the system, one can at least clarify the effect of lattice details and the effect of particular models of the lattice dynamics. It has been shown for the case of a diamond lattice that a particular choice of the intrinsic jump parameters for the local dynamics (as far as the set of elementary motions is capable of reproducing every conformational transition on a local scale) has no influence on the long time dynamic evolution of sufficiently long polymers below the glass transition density.^{19,20} On the other hand, the effect of the particular lattice itself can be to some extent examined by comparison of MC dynamic results from different lattice models.

In the present paper, we report on the results of dynamic MC studies of systems of long polymers confined to a simple cubic lattice. Since this lattice has a smaller persistence length than a diamond lattice, it should presumably also exhibit more dynamic flexibility. Thus, lattice chains composed of $n = 800$ segments on a five choice, cubic lattice should be equivalent to a considerably larger degree of polymerization in real polymers. Furthermore, the higher coordination number of a cubic, as compared to a diamond, lattice modifies the local interchain interactions and requires a different set of elementary motions, and thus another model of local dynamics. Unlike our previous work,^{19,20} we elected to study a wider range of chain lengths, thus, the present studies are limited to a single choice of polymer density, namely, $\phi = 0.5$. The largest system under consideration consists of $N = 40$ chains each of length $n = 800$. The $n = 800$ system is well above the largest chain length systems studied previously.^{21,22,31} The two main questions addressed in the present simulations are the following: First, is the dynamic behavior of the various lattice systems similar? Second, can we find a crossover to reptation dynamics when one considers a relatively long polymer?

In Sec. II we discuss the model of the dynamics employed. In Sec. III the equilibrium dimensions of model chains in the melt are briefly described and the excluded volume screening length is estimated. The major results of the present series of computational experiments are described in Sec. IV, where diffusion coefficients and terminal relaxation times are estimated and in Sec. V, where we show that the character of the polymer chain motion is quite different from the picture presented in reptation theory. Finally, a discussion of the results and some qualitative conclusions concerning the dynamics of polymer melts are given in Sec. VI.

II. MODEL OF THE DYNAMICS

The present model consists of a collection of monodisperse, nonintersecting chains confined to a five-choice cubic lattice. Since each of the N chains occupies n lattice vertices (connected by $n - 1$ "bonds", each of length $|l| = 1$) the volume fraction of the polymer is $\phi = N \cdot n / L^3$, where L is the size of MC box, with superimposed periodic boundary

conditions. The details of the method used to generate a high density system of long, self-avoiding polymers at thermal equilibrium can be found in our previous paper.¹⁹

It is well known for lattice chains with excluded volume that the set of elementary motions must be chosen to ensure that every possible conformational transition of a given part of the chain can be generated by a certain succession of these elementary motions.³²⁻³⁵ That is, there must be the local possibility of creating a new random conformation within the middle part of each chain. Otherwise, one may build in a n^3 relaxation scale into the model due to the fact that a new orientation of chain segments somewhere in the middle of the polymer can only be created by a "diffusion" of orientation from the ends.^{32,33} The following set of elementary motions seems to be effective (in that they have a large fraction of accepted jumps) and satisfies the abovementioned requirements for lattice dynamics. A superscript prime denotes a new orientation introduced by random selection among the possible outcomes.

(i) As schematically depicted in Fig. 1(A), we include "normal" bead motion, where $l_i, l_{i+1} \rightarrow l_{i+1}, l_i$, and chain end reorientations where $l_2 l_1 \rightarrow l'_2 l'_1$ (or $l_{n-2} l_{n-1} \rightarrow l'_{n-2}, l'_{n-1}$ at the opposite end).³⁶ Also shown is chain end motion where two end bonds are replaced by a new pair of randomly generated chain ends. There is also a small contribution from single bead modification of the chain ends when $l_2 = l'_2$ (or $l_{n-2} = l'_{n-2}$).

(ii) Three-bond (two-bead) permutations when $l_i, l_{i+1}, l_{i+2} \rightarrow l_{i+2}, l_{i+1}, l_i$ are schematically depicted in Fig. 1(B).³⁷ There exist several conformations which could be affected by this motion. Two of these involve diagonal motion of the bonds across a rectangle or a cube and the third produces a 180° flip of U-shaped structures.

(iii) The 90°-crankshaft motion effective only for a U-shaped fragment of the chain $l_i, l_{i+1}, l_{i+2} = l'_i, l_{i+1}, l'_{i+2}$ is depicted in Fig. 1(C).³⁴ These introduce new out-of-plane

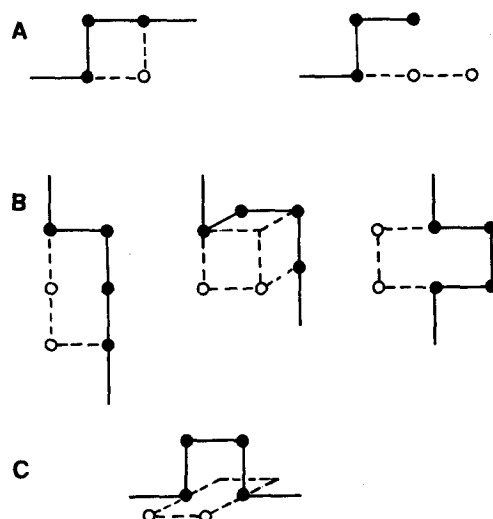


FIG. 1. (A) The normal bead motion and an example of chain end motion. (B) Examples of three-bond permutations. (C) The 90°-crankshaft motion of a U-shaped fragment of the chain.

orientations into the chain. The new orientation with $l'_i = -l'_{i+2}$ is selected from the two existing possibilities.

For every attempt at a particular kind of move (i)–(iii), the chain and the bond index (i) are selected by a random number generator. The time unit is defined as the time required for $(n-2)N$ attempts at a normal bead cycle, step (i), plus $(n-3)N$ attempts at a three-bond permutation cycle, step (ii), plus $(n-3)N$ attempts at a 90° crankshift cycle, step (iii), and finally $2N$, chain end cycles. Therefore, every polymer bead is subject to $1 + 2 + 2 = 5$ attempted motions, on average, per unit time. In practice, the sequence of the elementary motions are randomly mixed. Of course, any attempted elementary motion can be rejected for either (or both) of two reasons. First, the local conformation is not suitable; second, excluded volume restrictions prohibit the move. In Table I, the acceptance ratio for the various kinds of motions have been listed for systems of different chain lengths at the density under consideration ($\phi = 0.5$). The relatively low acceptance ratio for conformation changing, 90° flips (about 0.030) is quite sufficient to achieve locally, nonrestricted dynamics. Bond relaxation of any part of the chain (even in the case when $n = 64$) is a few orders of magnitude faster than the longest relaxation time of the chain. Therefore, the n^3 relaxation time scale due to nonphysical restricted dynamics^{32,33} is not artificially built into the model. The slight change of acceptance ratio with chain length is probably related to the changing relative contribution of the motion of the very end segments which are less restricted by chain conformation (or intrachain excluded volume); this effect anneals out with increasing n .

III. EQUILIBRIUM DIMENSIONS OF THE CHAIN

During the course of the dynamic MC simulations, the equilibrium properties of the system have been recorded. The values of various moments of the distribution function of the end-to-end vector \mathbf{R} , as well as of the radius-of-gyration vector, \mathbf{S} , are listed in Table II. First of all, one can note that the mean value of the magnitude of the radius-of-gyration $\langle |\mathbf{S}| \rangle$ of the polymer coil is always 3–5 times smaller than the size of the periodic MC box. Actually, even the average magnitude of the end-to-end vector $\langle |\mathbf{R}| \rangle$ is smaller than the box size, L by a factor of about 1.5. This allows us to reasonably assume that finite size effects on the measured equilibrium and dynamic properties are negligible. A brief inspection of the data in Table II shows that the chain length dependence of the coil dimensions are similar to those for an ideal chain. However, based on the ratio of the $\langle R^2 \rangle$ to the value for a five choice nonreversing random walk (NRRW)

on a cubic lattice $\langle R^2_{\text{NRRW}} \rangle$,³⁸ these chains are more expanded by a factor of 1.2–1.3. Similar behavior was seen in diamond lattice models.^{31,39,40} For instance, Kremer³¹ found even at the lower density, $\phi \approx 0.34$, that $\langle R^2 \rangle / \langle R^2_{\text{NRRW}} \rangle \approx 1.1$ for a diamond lattice system of $n = 200$ polymers. Thus, the local geometry may affect the interplay between the persistence length of the chain and the density of the system. Consequently, the quantitative dependence of the screening length on polymer density may be modified when one changes the particular lattice realization.

Other measured moments of the coil size (and the density within the coil) distribution exhibit a similar deviation from ideal chain behavior; however, the quasi-ideal scaling $\langle R^2 \rangle \sim \langle S^2 \rangle \sim (n-1)$ is satisfied with good accuracy. Since the equilibrium data for the case of $n = 800$ are less accurate than those for shorter chains (for the $n = 800$ case the sampling time in units of the terminal relaxation time is much shorter than for the $n = 216$ case) it is difficult to make definitive statements on the limiting ($n \rightarrow \infty$) values of the equilibrium properties of the chain in melt. However, the data for $n = 216$ (which are significantly more accurate) should be very close to that expected for very long polymers.

An approximate estimate of the screening length can be obtained by comparing the dimensions of the coil in the model melt with the dimensions of five-choice, cubic lattice, self-avoiding random walks (SAW's)—the model of a single polymer in good solvent. The scaling of the SAW data obtained from MC sampling by Rapaport⁴¹ give, respectively,

$$\langle R^2 \rangle_{\text{SAW}} = 1.134(n-1)^{1.184} \quad (1)$$

and

$$\langle S^2 \rangle_{\text{SAW}} = 0.1772(n-1)^{1.187} \quad (2)$$

This is to be compared with the least-square fit of the present results (Table II):

$$\langle R^2 \rangle = 1.984(n-1)^{0.987} \quad (3)$$

and

$$\langle S^2 \rangle = 0.2759(n-1)^{1.024} \quad (4)$$

Equating $\langle R^2 \rangle = \langle R^2 \rangle_{\text{SAW}}$ one obtains $n_B \approx 17$, and on setting $\langle S^2 \rangle = \langle S^2 \rangle_{\text{SAW}}$, $n_B \approx 15$, respectively. These estimates are consistent with the screening length found by the same method for a diamond lattice model at the same density.²⁰ Note that other approaches used in the estimation of the mesh size in an entangled polymer system lead to even lower values of n_B . Thus taking into account the upper value, $n_B \approx 17$ of the screening length, one obtains the blob diameter $\xi_B \approx 4.5$ from the NRRW formula³⁸ for the mean-square,

TABLE I. Fraction of accepted motions for cubic lattice chains at $\phi = 0.5$.^a

Type of motion	$n = 64$	$n = 100$	$n = 216$	$n = 800$
Two-bond permutations	0.3879(2)	0.3880(2)	0.3880(1)	0.3883(1)
Chain-end motions	0.2696(2)	0.2704(2)	0.2712(2)	0.2715(3)
Three-bond permutations	0.2387(1)	0.2391(2)	0.2392(3)	0.2395(2)
Three-bond, 90° , flips	0.0305(1)	0.0304(1)	0.0302(0)	0.0300(0)

^aThe number of parentheses indicates the uncertainty (90% confidence limit) of the last displayed digit.

TABLE II. Equilibrium dimensions of polymer chains at $\phi = 0.5$ (monodisperse system).

Property	$n = 64$	$n = 100$	$n = 216$	$n = 800$
	$N = 32$ $L = 16$	$N = 40$ $L = 20$	$N = 32$ $L = 24$	$N = 40$ $L = 40$
$\langle R \rangle$	9.91 ^a	12.71	18.86	35.15
$\langle R^2 \rangle$	115.1	187.2	413.4	1425
$\langle R^4 \rangle / \langle R^2 \rangle^2$	1.572	1.573	1.593	1.542
$\langle S \rangle$	4.26	5.42	8.01	15.69
$\langle S^2 \rangle$	19.06	30.77	67.48	258.4
$\langle S^4 \rangle / \langle S^2 \rangle^2$	1.190	1.203	1.224	1.210
$\langle R^2 \rangle / \langle R_{\text{NRRW}}^2 \rangle^b$	1.227	1.266	1.284	1.190

^a The statistical error (90% confidence limit) for $\langle |R| \rangle$ and $\langle |S| \rangle$ is below $\pm 1\%$, except for $n = 800$, where the error generally is about twice as large ($\pm 2\%$). For $\langle R^2 \rangle$ and $\langle S^2 \rangle$, the error is on the level of $\pm 1\%$, and for the fourth reduced moment, it is not greater than $\pm 3\%$ ($\pm 6\%$ for $n = 800$).

^b $\langle R_{\text{NRRW}}^2 \rangle$ is the mean-square end-to-end distance for a nonreversing random walk on a five-choice, cubic lattice and is given by $\langle R_{\text{NRRW}}^2 \rangle = \frac{2}{3}(n-1) - \frac{1}{3}[1 - (1/5)^{n-1}]$ (Ref. 38).

end-to-end vector of the blob, $\langle R^2 \rangle_{n_B}$, with the abovementioned prefactor of 1.2. When one compares ξ_B^2 with $\langle R^2 \rangle^{1/2}$ of the longer polymers studied here, it appears that every requirement of reptation theory concerning the range of ratios of n/n_B where reptation should dominate are satisfied.²⁴⁻²⁷ In particular for the $n = 800$ case, the ratio $n/n_B = 47$ if in fact n_B corresponds to the number of "static" blobs between entanglements.

IV. CENTER-OF-MASS MOTION AND RELAXATION OF THE END-TO-END VECTOR

The motion of the center-of-mass (CM) of the polymer chain is most simply discussed in the terms of the autocorrelation function $g_{\text{CM}}(t)$, which is the mean-square displacement of the center-of-mass obtained as an average over the trajectories of all the chains in the model system. The time course of $g_{\text{CM}}(t)$ vs t is plotted in Fig. 2 on a log-log scale.

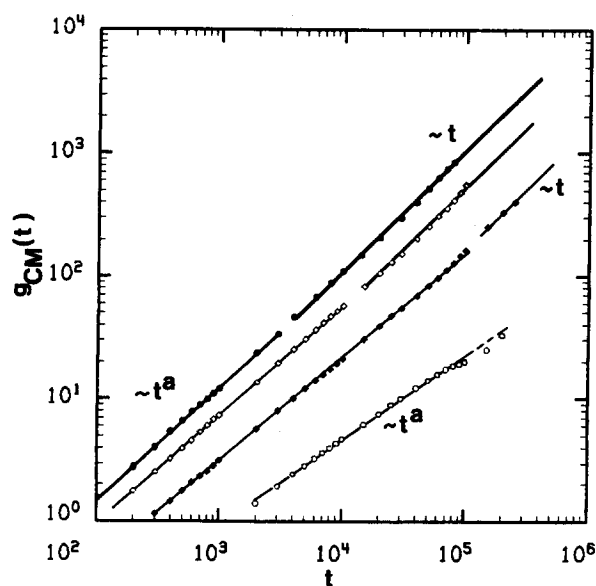


FIG. 2. Log-log plots of the center-of-mass autocorrelation function $g_{\text{CM}}(t)$ vs time t for $n = 64, 100, 216,$ and 800 reading from left to right (or top to bottom). $\phi = 0.5$ in all cases. The shorter time t^a regime is to be distinguished from the long time diffusion regime. Values of the exponent a are listed in row one of Table III.

There are clearly two time regimes of polymer motion. In the range $l^2 < g_{\text{CM}}(t) < 2\langle S^2 \rangle$, the autocorrelation function $g_{\text{CM}}(t)$ obeys the simple scaling relation $g_{\text{CM}}(t) \sim t^a$. The value of a for the various cases studied are exhibited in row one of Table III. This scaling is exact in the range of statistical accuracy, and there are no systematic deviations except very close to the vicinity of $2\langle S^2 \rangle$ where the t^a regime crosses over into the free diffusion limit, namely where $g_{\text{CM}}(t) \sim t$. Note that $\sqrt{2}\langle S^2 \rangle^{1/2}$ is precisely the distance over which the internal modes of a Rouse chain relax to their equilibrium values.²⁰ As the chain length increases, the exponent a decreases, presumably reflecting more and more constrained motion. The apparent (time-dependent) self-

TABLE III. Diffusion coefficients and terminal relaxation times for monodisperse systems and exponents for the autocorrelation functions in the intermediate time regime.

	$n = 64$	$n = 100$	$n = 216$	$n = 800$
a^a	0.909 ± 0.006	0.890 ± 0.001	0.839 ± 0.001	0.705 ± 0.006
D	1.66×10^{-3} $\pm (0.02 \times 10^3)$	9.03×10^{-4} $\pm (0.21 \times 10^{-4})$	2.64×10^{-4} $\pm (0.05 \times 10^{-4})$	(2.8×10^{-5}) (upper bound) (1.2×10^{-5}) (lower bound)
τ_R	1.95×10^3 $\pm (0.02 \times 10^3)$	6.05×10^3 $\pm (0.29 \times 10^3)$	4.74×10^4 $\pm (0.08 \times 10^4)$	(...)
$\frac{D\tau_R}{\langle R^2 \rangle}$	2.80×10^{-2}	2.92×10^{-2}	3.03×10^{-2}	(...)
b^b	0.540 ± 0.004	0.522 ± 0.004	0.481 ± 0.001	0.360 ± 0.008

^a Exponent in the $g_{\text{CM}}(t) \sim t^a$ relation; for $n = 800$, the upper limit of the displacement is slightly below $\langle S^2 \rangle$.

^b Exponent of $g(t) \approx t^b$ in the range $\xi_B^2/3 < g(t) < \langle S^2 \rangle$. For $n = 800$, the upper limit is slightly below $\langle S^2 \rangle$, and the lower limit is the point [$g(t) \approx 25$] when the slope of $\log[g(t)]$ vs $\log(t)$ initially decreases, and is approximately the value of the smallest slope. The average is taken over the entire chain for all the cases displayed here.

diffusion coefficient $D(t)$ obtained from the ratio $g_{\text{CM}}(t)/6t$ decreases with time over the t^a regime. This suggests that the center-of-mass motion couples into the internal modes of the various chains.

In our simulations up to $n = 216$, we observed the $g_{\text{CM}}(t) \sim t^a$ regime up to displacements in the range of $2\langle S^2 \rangle$. Since these cubic lattice chains are presumably equivalent to longer chains on a diamond lattice, we observe a stronger chain length dependence of a than was previously seen in the latter case. In particular, the $n = 800$ chain exhibits quite a significant decrease of a in comparison with the $n = 216$ case. The exponent $a = 0.839$ for the $n = 216$ polymers on a cubic lattice is less than that for the $n = 216$ chains on a diamond lattice case where $a = 0.90^{20}$ (the diamond lattice case appears to be essentially equivalent to an $n = 100$ chain on a cubic lattice).

The long time limits of the self-diffusion coefficients D compiled in Table III were estimated from the relation⁴²:

$$g_{\text{CM}}(t) = 6Dt + \text{constant}, \quad (5)$$

where the *constant* has a small positive value and reflects the faster motion over the initial t^a regime. The least-square fit was applied to the data for $g_{\text{CM}}(t) > 2\langle S^2 \rangle$. The upper limit of the value of $g_{\text{CM}}(t)$ is dictated by the requirements of good statistics (due to averaging over the trajectory) and was taken to be in the range of $10\langle S^2 \rangle$. For that value of $g_{\text{CM}}(t)$, at least 2×10^3 "chains" contributed to the average for the cases of $n = 64$ up to $n = 216$.

Unfortunately the above procedure cannot be directly applied to the data for $n = 800$ because we have not covered the equivalent time scale due to the extreme length of these computations. However, it is possible to make some predictions of the value of the diffusion coefficient even in this case. The upper bound for the self-diffusion coefficient is just the apparent time dependent diffusion coefficient estimated from the ratio $g_{\text{CM}}(t)/6t$ for times over the range of displacements studied. Since $D(t)$ decreases with time, the calculated value is always larger than those expected for times much longer than τ_R . Note that over the time window already studied ($n = 800$) the dynamic evolution of the system extends up to the time when the autocorrelation of the end-to-end vector $\langle \mathbf{R}(t) \cdot \mathbf{R}(0) \rangle$ decays to $2/3$ of its initial value and is in the terminal relaxation time regime, and therefore one would not expect any dramatic change in the character of the polymer motion at longer times [see, for example, Fig. 3(B)]. The lower bound for the diffusion coefficient in the case of $n = 800$ can be obtained from the assumption that the t^a regime extends up to $g_{\text{CM}}(t) = 2\langle S^2 \rangle$, by analogy to the shorter chain systems. The data for the $n = 800$ case obtained by the aforementioned considerations are listed in parentheses in row two of Table III in order to distinguish between values obtained from exact and approximate methods. This analysis, however, is probably not complete, due to some qualitative changes in the course of the single bead autocorrelation function which will be discussed in the next section.

Table III also contains the terminal relaxation times, τ_R , for the end-to-end vector autocorrelation function, as well as the ratio $D\tau_R/\langle R^2 \rangle$ for the system of interest. The

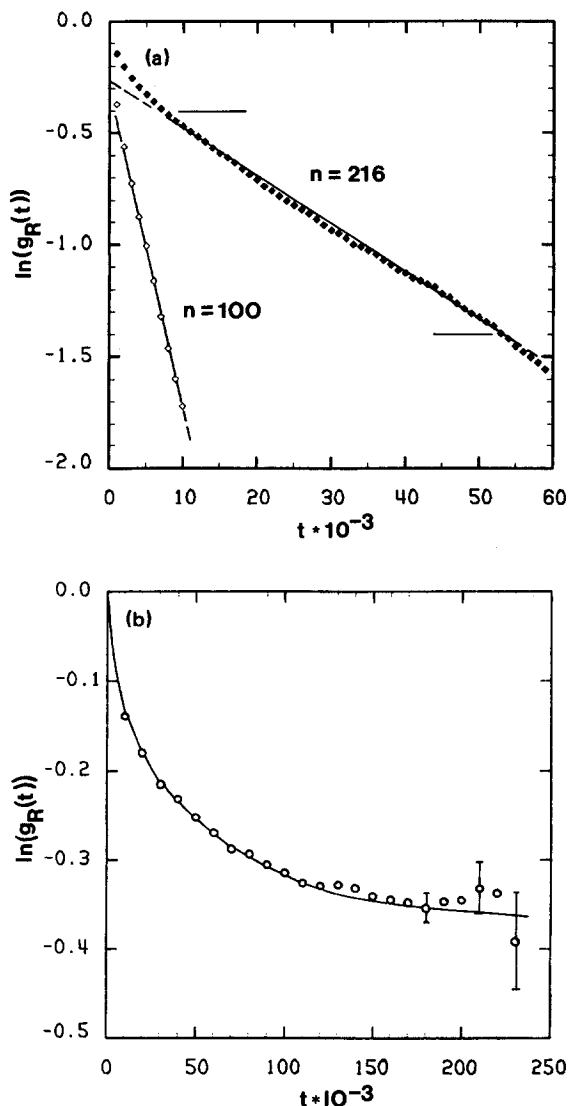


FIG. 3. (A) Plots of $\ln g_R(t)$ vs time t [$g_R(t) = \langle \mathbf{R}(t) \cdot \mathbf{R}(0) \rangle / \langle R^2 \rangle$] for $n = 100$ and $n = 216$, respectively. The horizontal bars indicate the region used for the least-square fit used for estimation of τ_R . (B) The plot of $\ln g_R(t)$ vs time for $n = 800$. In all cases $\phi = 0.5$.

relaxation times are obtained from least-square fits to the linear portion of the semilog plot of $g_R(t) = \langle \mathbf{R}(t) \cdot \mathbf{R}(0) \rangle / \langle R^2 \rangle$ vs t . Since there is a short period of very fast relaxation, a well defined window $-0.4 < \ln [g_R(t)] < -1.4$ has been chosen for the fitting procedure; the range of $g_R(t)$ fit to extract τ_R is similar to those used by other workers.^{34,43} Representative plots of $\ln g_R(t)$ vs t are given in Figs. 3(A) and 3(B).

The self-diffusion coefficient and longest relaxation time τ_R are well described by the following scaling (over the range $n = 64$ to $n = 216$):

$$D \sim n^{-1.52(\pm 0.06)} \quad (6)$$

and

$$\tau_R \sim n^{2.63(\pm 0.04)}. \quad (7)$$

However, there is a systematic deviation in the direction of a stronger dependence of D on n with increasing chain length,

with the deviations on the border of the statistical accuracy. Using the two points at $n = 100$ and $n = 216$, gives $D \sim n^{-1.60}$ and $\tau_R \sim n^{2.68}$. This trend in the exponents of D and τ_R is consistent with previous multichain cubic lattice simulations of chains up to $n = 48$ that have found a weaker dependence on n .⁴³ Note that the comparison of the diffusion coefficient for $n = 216$ with the very qualitative estimate for $n = 800$ case leads to $D \sim n^{-2.04 \pm 0.32}$.

The chain length effect on the scaling of D with n can be very qualitatively accounted for by a simple form of the type

$$D = c \cdot (n + n^2/n_e)^{-1}, \quad (8)$$

where the c and n_e are adjustable parameters. Physically c corresponds to the effective diffusion constant per bead in the absence of chain connectivity, and n_e is the mean distance between entanglements.⁴⁴ The above functional form gives $D \sim n^{-1}$ in the range of relatively short chains and crosses over to $D \sim n^{-2}$ in the limit of very long chains. The fit of the data in the window from $n = 64$ to $n = 216$ gives n_e in the range of 125, and an extrapolation to $n = 800$ gives $D_{800} = 2.73 \times 10^{-5}$, which is essentially the "experimental" upper bound (see Table III) for this quantity. Since the "true" diffusion coefficient for the $n = 800$ polymer is likely to be somewhat lower, one might expect to find a somewhat lower value of n_e when the data for longer chains become available. This consideration, however qualitative, indicates that the static and dynamic entanglement lengths may differ by at least an order of magnitude, as has been suggested by other workers.^{21,31}

As implied by the data in row four of Table III, the product $D\tau_R$ from the present simulation scales vs n with an exponent of about 1.1. This appears to be a real effect (note that $\langle R^2 \rangle$ and $\langle S^2 \rangle$ scale essentially as n , see Table II); however, the exponent of $D\tau_R$ found here is smaller than the value 1.2 found for the diamond lattice in Ref. 20. We should note that all the scaling behaviors found here for the cubic lattice model are very close (within essentially the same range of uncertainties) to those seen in the diamond lattice model simulations at the same density $\phi = 0.5$ and over the same range of chain lengths.²⁰ Therefore, it is important to examine if the qualitative character of the long-distance motion of the polymer (especially for the $n = 800$ chain) is consistent with the picture presented in previous work. We might again point out that although the time scale covered by the simulation for $n = 800$ is below the diffusion time for entire chain, it is sufficient to examine whether or not these chains are reptating.

V. ANALYSIS OF SINGLE BEAD MOTION AND THE PRIMITIVE PATH

The average mean-square displacement of the single beads of the model chains, $g(t)$, is plotted in a log-log scale in Fig. 4 against time. The averaging of $g(t)$ is performed over the entire chain length. There is simple Rouse-like behavior of the system up to $n = 216$. The slope of $\log g(t)$ vs $\log(t)$ in the well defined regime t^b which extends up to $\langle S^2 \rangle$, changes gradually from 0.54 for $n = 64$ to 0.48 for $n = 216$. The values of b are compiled in row five of Table III. If one considers only the middle part of the chain, the

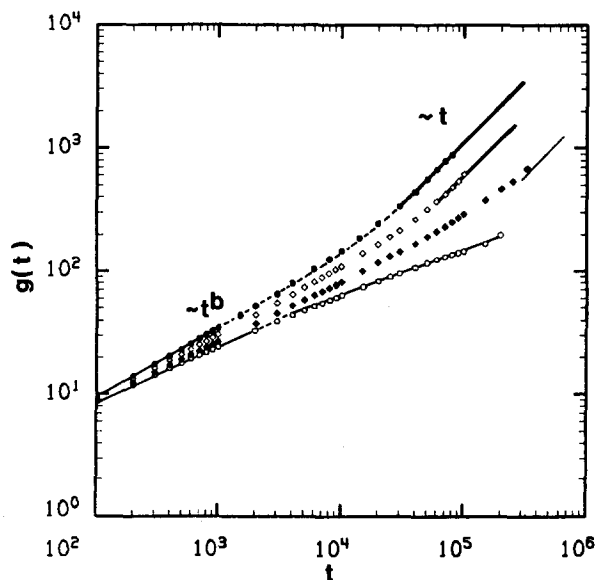


FIG. 4. Log-log plots of the single bead autocorrelation function $g(t)$ vs time t for $n = 64, 100, 216,$ and 800 reading from top to bottom. The $g(t)$ are averaged over all the beads in the system. The shorter time t^b regime exponents (the plateau exponent for $n = 800$) are listed in row five of Table III. In all cases $\phi = 0.5$.

case of $n = 100$ seems to exhibit the behavior equivalent to chains of length $n = 216$ on a diamond lattice examined in previous work.²⁰

The $n = 800$ case exhibits some qualitative changes in behavior. There is clearly a decreased slope, with a minimum value of 0.36. This presumably reflects the more constrained dynamics of these very long chains. Phenomenologically, this might appear to be similar to the $t^{1/4}$ regime predicted by reptation theory.¹⁻⁴ However, the microscopic picture that emerges is rather different.

The analysis of the primitive path motion of the chain contour has been performed in a similar manner as in previous work.²⁰ First, we constructed the equivalent primitive path for every chain at a given time taken here to be zero time. Every bead of the original chain has been replaced by a virtual point on the equivalent path which is the center-of-mass of the blob composed of $n_B = 17$ beads [see Fig. 5(A)]. Thus we obtained a relatively smooth path composed of partially overlapping blobs. Second, we then compute the average displacement down the primitive path. The basic idea is schematically presented in Fig. 5(B). The average value of the mean number of steps ($i - j$) down the primitive path after a time t was computed over the central one quarter of the path. The reptation component is then estimated as

$$g_{\parallel}(t) = l_p^2 \langle (\overline{i-j})^2 \rangle, \quad (9)$$

where the bar denotes that the value of $i - j$ is averaged over a given chain, the $\langle \rangle$ indicates that a further averaging is performed over the entire collection of chains, and l_p^2 is the mean-square-length of the segment of the primitive path (about 0.103 in the present model). The remaining, transverse component of the motion of the primitive path is estimated after elimination of the curvilinear component as

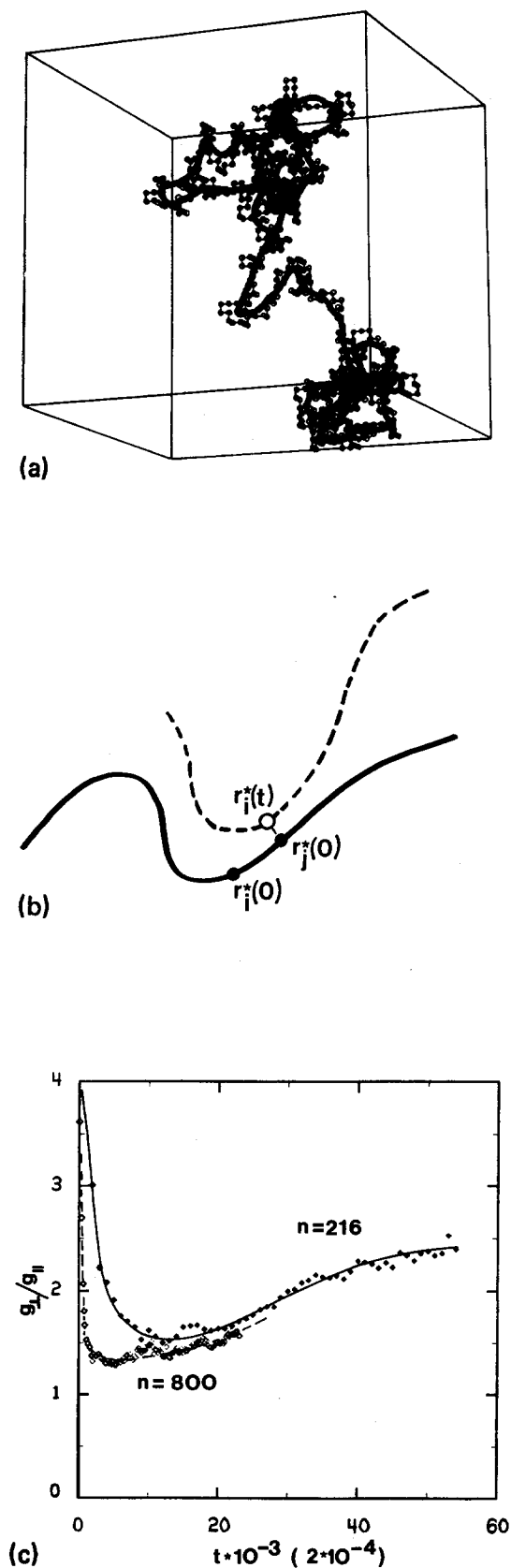


FIG. 5. (A) Snapshot of the original chain (open symbols) and the equivalent path (heavy solid line) of a chain with $n = 800$, $n_B = 17$. (B) The projection of the equivalent chain coordinates at time t , $r_i^*(t)$ onto the initial state of the equivalent chain at zero time, $r_i^*(0)$. (C) The plot of the ratio $g_{\perp}(t)/g_{\parallel}(t)$ vs time for $n = 216$ (upper curve) and $n = 800$ (lower curve). See the text for more details.

$$g_{\perp}(t) = \langle (r_j^*(0) - r_i^*(t))^2 \rangle, \quad (10)$$

where $r_j^*(0)$ and $r_i^*(t)$ are the coordinates of the j th and i th bead of the equivalent chain at the relevant times. The averaging involves all the paths and includes the middle segment of the chain twice the length of that used to calculate the $(i-j)$ shift [the net displacement $(i-j)$ can be either positive or negative]. Therefore, the procedure is valid for $|i-j| \leq n/4$, and has been applied only to the equivalent range of times. In Fig. 5(C), the ratio $g_{\perp}(t)/g_{\parallel}(t)$ is plotted against time for $n = 216$ and $n = 800$ chains in the solid and open diamonds, respectively. The essential features are the same as observed previously.²⁰ At very short times, there is significant preference for transverse motion due to the interplay of chain connectivity and the excluded volume effect. Then there is a short period of time when the motion down the chain becomes relatively more important (the minimum on the curves) at distances on the order of the blob size (or equivalently, the estimated tube diameter). Finally, the longitudinal component increasingly becomes less and less important, with the transverse component increasing much faster with time. As a result, the ratio g_{\perp}/g_{\parallel} again increases. Therefore, one may conclude that reptation-like fluctuations down the tube are strongly damped. Apparently, the fast contribution of the reptation mode dies on a distance comparable to the mesh size. As a result, the motion of the points on the equivalent chain is essentially isotropic. Note that the times considered are below the tube renewal time of the reptation theory; therefore, if these model polymers indeed reptated, the ratio $g_{\perp}/g_{\parallel}(t)$ should have monotonically decreased with time.

It is most instructive to examine the character of the motion (especially in the case of $n = 800$) of the chain in the melt. Snapshot pictures of the chain conformation at various times may be very useful for that purpose. Since the $n = 800$ polymer is very long, the primitive path based on the $n_B = 17$ approximation is generally a very complicated, entangled three-dimensional structure. Therefore, for clarity of graphical presentation we generated much smoother equivalent paths where the averaging of the original chain was performed over $n_B = 101$ neighboring (down the chain) beads. This approach may also meet the postulate that the dynamic entanglement length is larger than the static one. In Figs. 6(A)–6(C), the dynamic evolution of a single $n = 800$ chain in the melt is presented. The thinner lines represent the configuration of the equivalent path at the initial time and the solid circles the equivalent path at a time t later. After a time t of 6×10^4 , 1.2×10^5 , and 2×10^5 as clearly depicted in Figs. 6(A)–6(C), significant transverse fluctuations are evident even when the definition of the equivalent chain ($n_B = 101$) is very conservative. Again, the motion down the original path is hardly noticeable, an effect partially due to the long subchain used to generate the average conformation. As was mentioned above, the fast longitudinal motion has a rather local character. In other words, there is a short distance motion of the “defects” down the chain, however, it is not accompanied by substantial sliding of the entire chain down the primitive path. In Figs. 7(A)–7(C) we display snapshot projections of some other chains at a single time

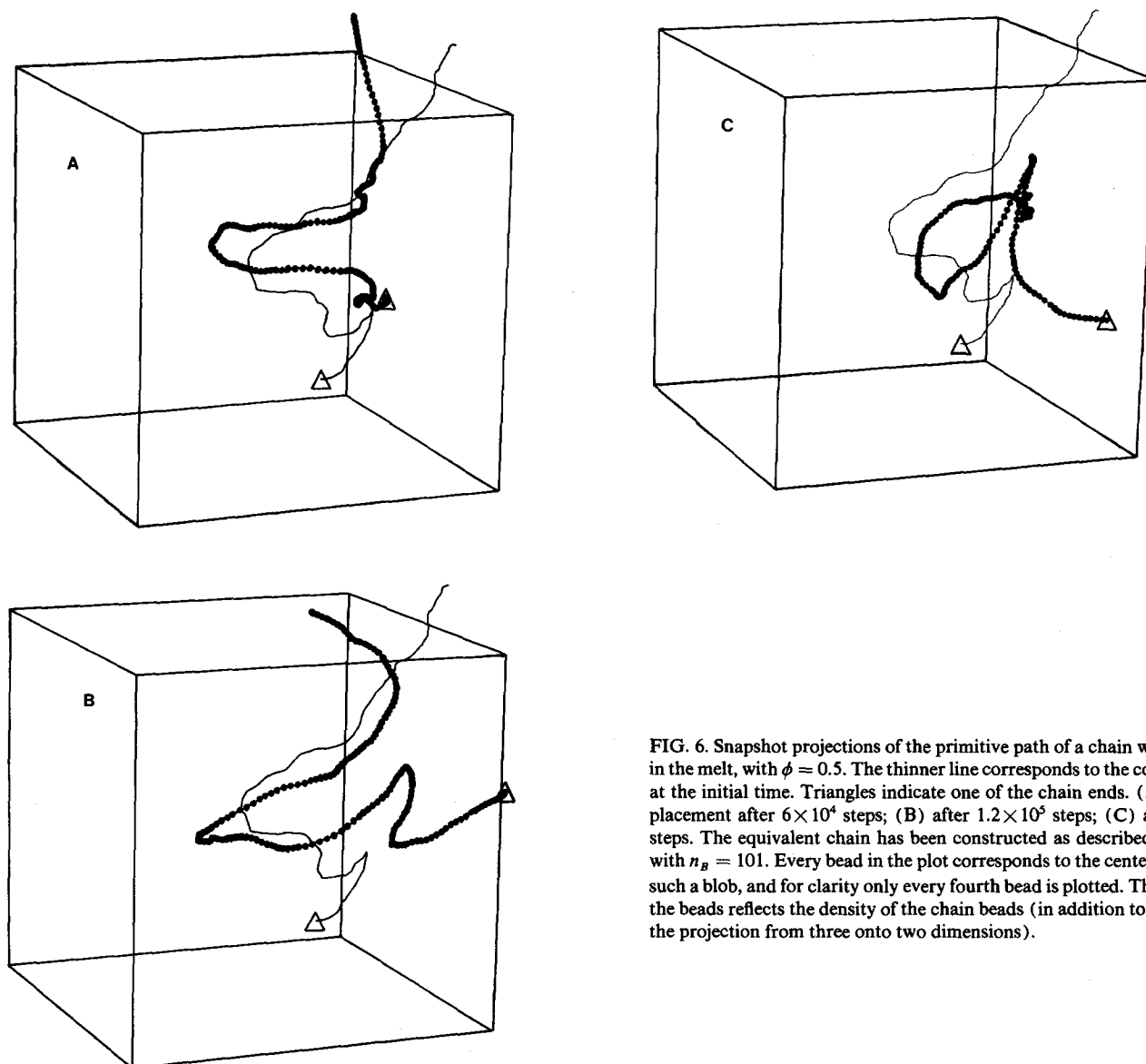


FIG. 6. Snapshot projections of the primitive path of a chain with $n = 800$ in the melt, with $\phi = 0.5$. The thinner line corresponds to the conformation at the initial time. Triangles indicate one of the chain ends. (A) The displacement after 6×10^4 steps; (B) after 1.2×10^5 steps; (C) after 2×10^5 steps. The equivalent chain has been constructed as described in the text with $n_B = 101$. Every bead in the plot corresponds to the center-of-mass of such a blob, and for clarity only every fourth bead is plotted. The density of the beads reflects the density of the chain beads (in addition to the effect of the projection from three onto two dimensions).

$t = 1.2 \times 10^5$ (somewhat below one-half the time of the entire run for the $n = 800$ system). The choice of chains is representative. Again, the motion of the chain seems to be isotropic, with an apparent local preference for transverse motion. Equivalent chains were generated in the same way as in Fig. 6.

VI. DISCUSSION

The present work shows that there is no qualitative difference between the dynamics of multichain systems confined to various lattices. Since there are some quantitative differences at the same n in the static properties of the diamond lattice system we formerly studied and the present simple or cubic lattice system, we conclude that cubic lattice chains at a given n correspond to somewhat longer real polymers. Comparison of the persistence length and the screening length of excluded volume suggests a factor of about 2 in n between the cubic and diamond lattices. Therefore, the present simulations of $n = 216$ and $n = 800$ significantly ex-

tend all the previous computer experiments on multichain polymer systems^{20-22,31,43,45,46} to a far more entangled regime. Indeed, we have observed for the first time at fixed ϕ the indication of the crossover in $D \sim n^{-\alpha}$ from a smaller exponent α equal to unity to the larger value of two typical for a polymer melt of long chains. A previous study of the cubic lattice system up to $n = 48$ by Crabb and Kovac⁴³ suggested an exponent of $\alpha = 1.2-1.25$ at $\phi = 0.5$ (interpolated). Our system for $n = 64-100$ gives $\alpha \cong 1.4$, for $n = 100-216$ $\alpha \cong 1.6$, and finally a rather conservative estimate for the range $n = 216-800$ gives $\alpha = 2.04 \pm 0.32$. The above comparison shows that the crossover is relatively smooth, occurring over quite a broad range of chain length.

It is difficult to answer the question of to what extent the exponent in the smaller n regime is consistent with experiment.²⁴ Certainly, there has to be this kind of crossover in real systems. However, there is a paucity of experimental data in the crossover regime. Moreover, the effect of a particular lattice in the short chain limit and the absence of hydrodynamic interactions in our simulations may cause a sub-

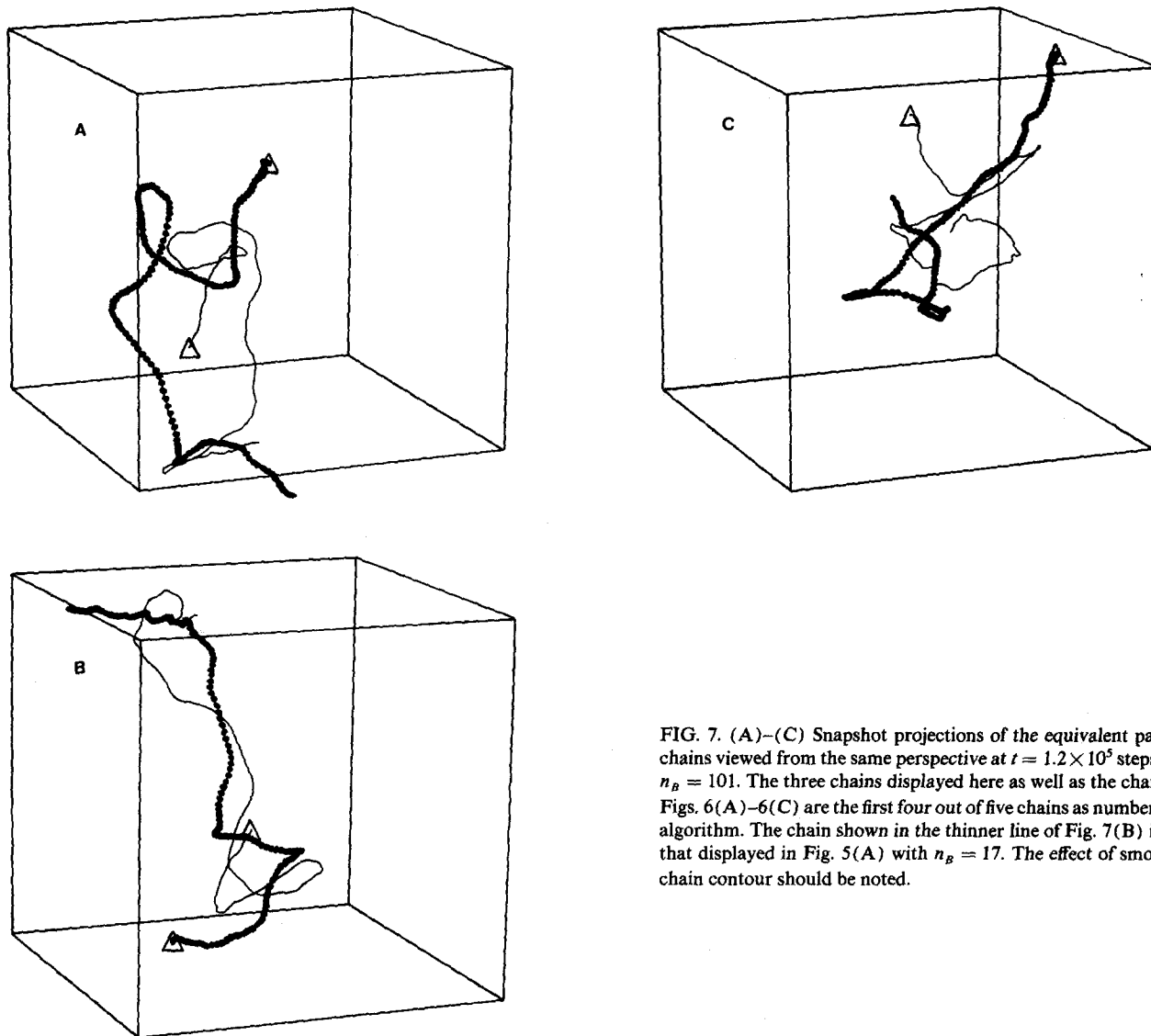


FIG. 7. (A)–(C) Snapshot projections of the equivalent path of various chains viewed from the same perspective at $t = 1.2 \times 10^5$ steps. In all cases, $n_B = 101$. The three chains displayed here as well as the chain depicted in Figs. 6(A)–6(C) are the first four out of five chains as numbered in the MC algorithm. The chain shown in the thinner line of Fig. 7(B) is the same as that displayed in Fig. 5(A) with $n_B = 17$. The effect of smoothing of the chain contour should be noted.

stantial difference between the real physical system and the model ones treated here. We further note that the excluded volume effect (static) is screened out at chain lengths much lower than those where the crossover to $D \sim n^{-2}$ behavior occurs. Therefore, the dynamic properties of the melt saturate in the limit of long chains at much higher values of n at a given density than do the static properties. Based on the fact that the longer chain lengths studied apparently crossover to the n^{-2} regime at intermediate densities these systems may be closer to the case of a concentrated solution than a melt, and therefore, the role of solvent quality may be of some importance.

With the above caveats in mind, nevertheless, the present simulations are qualitatively consistent with the crossover observed in real polymer melts from Rouse-like diffusion behavior to a more dynamically constrained regime where $D \sim n^{-2}$. The n^{-2} scaling has commonly been ascribed to the onset of reptation dynamics. However, the analysis of the dynamic evolution of the chain contour (the equivalent primitive path) shows that there is no well-

defined tube; rather, the motion of the system is essentially isotropic. The strong coupling of the motion of the various chains leads to the stronger chain length dependence of the self-diffusion coefficient and terminal relaxation times of the chain conformation. In other words, the separation of time scales for the motion of a single chain and for the motion of the surrounding media (composed of identical chains) crucial to the validity of reptation is not effective. When combined with previous simulations of diamond lattice systems at higher concentrations,²⁰ the present results show that the crossover to $D \sim n^{-2}$ with increasing concentration or with increasing chain length is not accompanied by a transition to the reptation mechanism of chain motion. Furthermore, it is worth noting that our lattice simulations exhibit qualitative agreement with previous MC experiments on off-lattice systems.^{45,46} In this context, it would be very interesting to see if those systems also show a similar character in the chain contour motion. Finally, let us note that the exponent α may not necessarily be equal to two over the entire entangled chain regime. Our simulations suggest that the particular numeri-

cal value of α may be dependent on various characteristics of the polymer system (e.g., the density, and perhaps the distance from the glass transition temperature, etc.).

We hope to get some additional insight into the mechanism of polymer diffusion in a melt from model studies of probe polymer motion in a matrix of chains having a different degree of polymerization. This forms the subject of the second part of this work (see following paper). An analytic theory which does not invoke the existence of reptation as the dominant mode of melt motion will also be presented in the near future.

ACKNOWLEDGMENTS

This research was supported in part by a grant from the Polymer Program of the National Science Foundation (No. DMR-85-20789). Acknowledgment is made to the Monsanto Company for an institutional research grant for the purchase of two μ VAX-II computers on which the simulations reported here were predominantly carried out.

- ¹P. G. de Gennes, *Phys. Today* **36**, No. 6, 33 (1983).
- ²P. G. de Gennes, *Scaling Concepts in Polymer Physics* (Cornell University, Ithaca, New York, 1979).
- ³P. G. de Gennes, *J. Chem. Phys.* **55**, 572 (1971).
- ⁴M. Doi and S. F. Edwards, *J. Chem. Soc. Faraday Trans. 2* **74**, 1789, 1802, 1818 (1978); **75**, 38 (1978).
- ⁵J. Klein, *Nature* **271**, 143 (1978).
- ⁶R. Kimmich and R. Bachus, *Colloid Polym. Sci.* **260**, 586 (1982); *Polymer* **24**, 964 (1983).
- ⁷G. Fleischer, *Polym. Bull.* **9**, 152 (1983); **11**, 75 (1984).
- ⁸J. Klein, D. Fletcher, and L. J. Fetters, *Nature (London)* **304**, 526 (1983).
- ⁹C. R. Bartels, B. Crist, and W. W. Graessley, *Macromolecules* **17**, 270 (1984).
- ¹⁰J. A. Wesson, I. Noh, T. Kitano, and H. Yu, *Macromolecules* **17**, 782 (1984).
- ¹¹P. F. Green, C. J. Palmstrom, J. W. Mayer, and E. J. Kramer, *Macromolecules* **18**, 501 (1985).
- ¹²P. F. Green, P. J. Mills, C. J. Palmstrom, J. W. Mayer, and E. J. Kramer, *Phys. Rev. Lett.* **53**, 2145 (1984).
- ¹³M. A. Antonietti, J. Coutandin, and H. Sillescu, *Macromolecules* **19**, 793 (1986).
- ¹⁴P. F. Green and E. J. Kramer, *Macromolecules* **19**, 1108 (1986).
- ¹⁵H. Kim, T. Chang, J. M. Yohanan, L. Wang, and H. Yu, *Macromolecules* **19**, 2737 (1986).
- ¹⁶G. C. Berry and T. G. Fox, *Adv. Polym. Sci.* **5**, 261 (1968).
- ¹⁷J. D. Ferry, *Viscoelastic Properties of Polymers* (Wiley, New York, 1980).
- ¹⁸G. D. J. Phillies, *Macromolecules* **19**, 2367 (1986).
- ¹⁹A. Kolinski, J. Skolnick, and R. Yaris, *J. Chem. Phys.* **84**, 1922 (1986).
- ²⁰A. Kolinski, J. Skolnick, and R. Yaris, *J. Chem. Phys.* **86**, 1567 (1987).
- ²¹A. Baumgartner, *Annu. Rev. Phys. Chem.* **35**, 419 (1984).
- ²²A. Baumgartner, in *Applications of the Monte Carlo Method in Statistical Physics* (Springer, Heidelberg, 1984).
- ²³S. G. Whittington, *Advances in Chemical Physics* (Wiley, New York, 1982), Vol. 51, Chap. 1, and references therein.
- ²⁴J. Klein, *Macromolecules* **11**, 852 (1978).
- ²⁵J. Klein, *Macromolecules* **19**, 105 (1986).
- ²⁶M. Daoud and P. G. de Gennes, *J. Polym. Sci., Polym. Phys. Ed.* **17**, 1971 (1979).
- ²⁷W. W. Graessley, *Adv. Polym. Sci.* **16**, 1 (1974); **47**, 67 (1982).
- ²⁸S. F. Edwards, *Polymer* **6**, 143 (1977).
- ²⁹P. E. Rouse, *J. Chem. Phys.* **21**, 1272 (1953).
- ³⁰H. Yamakawa, *Modern Theory of Polymer Solutions* (Harper and Row, New York, 1969), Chap. VI.
- ³¹K. Kremer, *Macromolecules* **16**, 1632 (1983).
- ³²H. J. Hilhorst and J. M. Deutch, *J. Chem. Phys.* **63**, 5153 (1975).
- ³³H. Boots and J. M. Deutch, *J. Chem. Phys.* **67**, 4608 (1977).
- ³⁴M. T. Gurler, C. C. Crabb, D. M. Dahlin, and J. Kovac, *Macromolecules* **16**, 398 (1983).
- ³⁵C. Stokely, C. C. Crabb, and J. Kovac, *Macromolecules* **19**, 860 (1986).
- ³⁶P. H. Verdier and W. H. Stockmayer, *J. Chem. Phys.* **36**, 227 (1962).
- ³⁷P. Romiszowski and W. H. Stockmayer, *J. Chem. Phys.* **80**, 485 (1984).
- ³⁸C. Domb and M. E. Fisher, *Proc. Cambridge Philos. Soc.* **54**, 48 (1958).
- ³⁹F. T. Wall and W. A. Seitz, *J. Chem. Phys.* **67**, 3722 (1977).
- ⁴⁰J. G. Curro, *Macromolecules* **12**, 463 (1979).
- ⁴¹D. C. Rapaport, *J. Phys. A* **18**, 113 (1985).
- ⁴²K. E. Evans and S. F. Edwards, *J. Chem. Soc. Faraday Trans. 2* **77**, 1891, 1929 (1981).
- ⁴³C. C. Crabb and J. Kovac, *Macromolecules* **18**, 1430 (1985).
- ⁴⁴A detailed analysis of the nature of dynamic entanglements will be presented in a forthcoming paper in the context of an analytic theory of melt dynamics. The qualitative result that emerges from the simulations described there is that there are a few long-lived contacts between pairs of blobs that belong to different chains. During the lifetime of these contacts, the pair diffuses through the melt; i.e., they are not static as reptation theory implies.
- ⁴⁵A. Baumgartner and K. Binder *J. Chem. Phys.* **75**, 2994 (1981).
- ⁴⁶M. Bishop, D. Ceperley, H. L. Frisch, and M. H. Kalos, *J. Chem. Phys.* **76**, 1557 (1982).